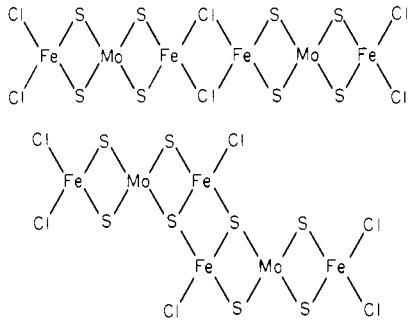

**Figure 5.** Possible structures for the $[MS_4Fe_2Cl_3^{2-}]_2$ anions.

VII). The first wave was diffusion controlled with a current function of 17 $\mu A/(V/s)^{1/2}$ mM, which at the HMDE corresponds to one electron. No reverse peak was seen for this wave. The heights of the second and third waves together corresponded to about one electron. An anodic wave was observed at +0.17 V vs. SCE. The additional cathodic waves that are observed in the voltammetry of $[Cl_2FeS_2WS_2FeCl_2]^{2-}$ appear to correspond to the waves observed in the reduction of $[MoS_4Fe_2Cl_3]^{2-}$. A likely interpretation of these results would be that the initial trianionic reduction product $[Cl_2FeS_2WS_2FeCl_2]^{3-}$ undergoes a much faster decomposition to $[WS_4Fe_2Cl_3]^{2-}$ than the molybdenum analogue. The difference of the peak potentials (240 mV) for the cathodic waves of the $[Cl_2FeS_2MS_2FeCl_2]^{2-}$ complexes (for M = Mo vs. W) supports the contention that the reduction is centered primarily on the molybdenum or tungsten atoms and is consistent with the Mössbauer data.

A possible structure for the $[MS_4Fe_2Cl_3]^{2-}$ complex anions must account for (a) the apparent dimeric nature of this compound suggested by the electrochemical results, (b) the bridging nature of the $MS_4$ group suggested by the infrared spectrum, and (c) the facile conversion to $[Fe(MoS_4)_2]^{3-}$ in coordinating solvents such as NMF. Two possible structures that are in compliance with the above restrictions are shown in Figure 5. Both of these structures contain two diffrent iron sites. The presence of single quadrupole doublets in the Mössbauer spectra of salts of the $[MS_4Fe_2Cl_3]^{2-}$ anions suggests either that the structures of $I^-$ and $II^-$ are different from any of those shown in Figure 5 or that the electronic differences between the two iron sites are too small to be resolved into two quadrupole doublets in the Mössbauer spectrum. The latter situation prevails in the Mössbauer spectra of structurally characterized mixed-ligand cubanes such as $[Fe_4S_4(SPh)_2Cl_2]^{2-}$ and $[Fe_4S_4(OPh)_2Cl_2]^{2-}$ that display only one quadrupole doublet in the Mössbauer spectra.[50]

**Acknowledgment.** This work has been supported generously by grants from the National Science Foundation (CHE-79-0389) and the National Institutes of Health (GM-26671-02).

**Registry No.** I, $Ph_4P$ salt, 73621-80-4; I, $Bu_4N$ salt, 88548-85-0; I, $Et_4N$ salt, 88562-92-9; $I^-$, $Et_4N$ salt, 88548-81-6; II, $Ph_4P$ salt, 73621-82-6; II, $Et_4N$ salt, 88562-93-0; $II^-$, $Et_4N$ salt, 88548-83-8; $(Ph_4P)_2(Cl_2FeS_2MoS_2)$, 88548-73-6; $(Ph_4P)_2(Cl_2FeS_2WS_2)$, 88548-75-8; $(Ph_4P)_2[(PhS)_2FeS_2MoS_2]$, 88548-77-0; $(Ph_4P)_2[(PhS)_2FeS_2WS_2]$, 73493-04-6; $(Ph_4P)_2(Br_2FeS_2MoS_2FeBr_2)$, 88548-79-2.

**Supplementary Material Available:** Listings of positional and thermal parameters for all atoms and observed and calculated structure factors and a stereo drawing of the unit cell contents (76 pages). Ordering information is given on any current masthead page.

(50) Kanatzidis, M.; Coucouvanis, D.; Simopoulos, A.; Kostikas, A., manuscript in preparation.
(51) Johnson, C. K. "ORTEP", Report ORNL-3794; Oak Ridge National Laboratory: Oak Ridge, TN, 1965.

Contribution from the Department of Chemistry, Indiana University, Bloomington, Indiana 47405, and Department of Chemistry and Laboratory for Molecular Structure & Bonding, Texas A&M University, College Station, Texas 77843

# Theoretical and Experimental Studies of the Electronic Structure of the $Mo_3(\mu_3\text{-}O)(\mu_3\text{-}OR)(\mu\text{-}OR)_3(OR)_6$ Type of Triangular Metal Atom Cluster Compound

MALCOLM H. CHISHOLM,*[1a] F. ALBERT COTTON,*[1b] ANNE FANG,[1b] and EDWARD M. KOBER[1a]

*Received June 16, 1983*

The electronic structure of a $Mo_3(\mu_3\text{-}O)(\mu_3\text{-}OR)(\mu\text{-}OR)_3(OR)_6$ molecule with R = H and $C_{3v}$ symmetry, which serves as a model for real molecules in which R = $CH_2C(CH_3)_3$ or $CH(CH_3)_2$, has been calculated by the molecular orbital method of Hall and Fenske. The calculations have been performed not only on the entire molecule but on the $Mo_3^{12+}$, $Mo_3O(OH)^{9+}$, and $Mo_3O(OH)_4^{6+}$ fragments, and the metal–metal bonding has been tracked through these successive stages by the "clusters in molecules" formalism. In the full molecule the HOMO is an e orbital that carries most of the e-type M–M bonding while the $a_1$ type is carried by two MO's, one of which is quite stable. The LUMO is also an e-type orbital and the HOMO–LUMO gap is small (ca. 1.5 eV). It is predicted that the $Mo_3O(OR)_{10}$ molecules of this type will have readily accessible redox chemistry in which both oxidation and reduction steps might be slow or irreversible, judging by the character of the HOMO and LUMO of the $Mo_3O(OR)_{10}$ molecule. Experimental observations on $Mo_3O(ONe)_{10}$, Ne = $CH_2C(CH_3)_3$, are in harmony with this. In addition, the absorption spectrum of $Mo_3O(ONe)_{10}$ has been observed, and an assignment based on the calculations is proposed.

## Introduction

The group 6 elements molybdenum and tungsten show a remarkable predilection to form equilateral triangular metal atom cluster compounds,[2] and such clusters are also formed by other early transition elements[3] such as niobium.[4] Previous studies by Cotton and co-workers, in collaboration with colleagues in Haifa and Jerusalem, have provided experimental data as well as theoretical analyses[2,5] of compounds of the form $[M_3(\mu_3\text{-}X)_2(O_2CR)_6L_3]$, $[M_3(\mu_3\text{-}X)(\mu\text{-}Y)_3L_9]$, and $[M_3(\mu_3\text{-}X)(O_2CR)_6L_3]$. Theoretical work has also been done on related systems.[6,7]

(1) (a) Indiana University. (b) Texas A&M University
(2) For extensive references to earlier work both here and elsewhere, see ref 1–10 in: Ardon, M.; Cotton, F. A.; Dori, Z.; Fang, A.; Kapon, M.; Reisner, G. M.; Shaia, M. *J. Am. Chem. Soc.* **1982**, *104*, 5394.
(3) Müller, A.; Jostes, R.; Cotton, F. A. *Angew. Chem.* **1980**, *92*, 921; *Angew. Chem., Int. Ed. Engl.* **1980**, *19*, 875.
(4) Bino, A. *J. Am. Chem. Soc.* **1980**, *102*, 7990.
(5) Bursten, B. E.; Cotton, F. A.; Hall, M. B.; Najjar, R. C. *Inorg. Chem.* **1982**, *21*, 302.
(6) Cotton, F. A.; Fang, A. *J. Am. Chem. Soc.* **1982**, *104*, 113.
(7) Fang, A. Ph.D. Dissertation, Texas A&M University, 1982.

0020-1669/84/1323-0749$01.50/0 

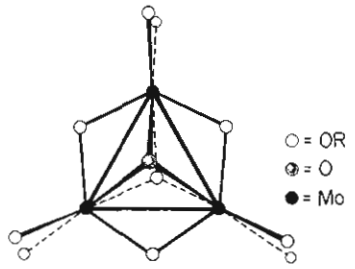


**Figure 1.** Schematic representation of the type of structure occurring in the $Mo_3(\mu_3\text{-}O)(\mu_3\text{-}OR)(\mu\text{-}OR)_3(OR)_6$ compounds.

In 1981, Chisholm and co-workers[8] reported the existence of yet another structural type (Figure 1) of trinuclear molybdenum(IV) cluster compound. We have employed the compound $Mo_3O(ONe)_{10}$, where Ne represents the neopentyl group, $(CH_3)_3CCH_2$, to conduct experimental studies of this molecule and the anion $[Mo_3O(ONe)_{10}]^-$ bearing on the electronic structures of such species. We have also carried out a theoretical analysis of $Mo_3O(OH)_{10}$ as a model of this type of compound, employing the Fenske–Hall[9] method of calculation, to see how the bonding here would compare with that in the three types of cluster compounds previously treated and to see if an understanding of the redox chemistry and absorption spectrum of this type of cluster could be achieved. The results are reported and discussed here.

## Experimental and Computational Procedures

The Fenske–Hall calculations were carried out in a manner previously described in detail.[5-7] The structural parameters reported by Chisholm et al.[8] were idealized to $C_{3v}$ symmetry, and the OR groups were replaced by OH.

Standard experimental techniques for the manipulation of the air- and water-sensitive materials were employed. The compound $Mo_3O(ONe)_{10}$ was prepared as previously described.[8] Electronic absorption spectra were obtained with a Hitachi 330 recording spectrophotometer. Samples were run vs. a solvent blank using matched 1-cm or 1-mm quartz cells. The cyclic voltammograms were obtained with use of a PAR 173 potentiostat, a PAR 175 programmer, and a Houston 2000 X-Y recorder. A three-compartment cell was used with a platinum-bead or -gauze working electrode, a platinum-wire auxiliary electrode, and a Ag/AgCl pseudoreference electrode. A 0.2 M solution of tetra-*n*-butylammonium hexafluorophosphate (TBAH) was employed as supporting electrolyte. No internal resistance compensation was used. Scan rates were 200 mV/s. EPR measurements (X band) were made on a Varian E-3 spectrophotometer.

## Results and Discussion

**Calculations.** We shall first examine the theoretical picture of the bonding provided by the calculations and then analyze the experimental observations in light of this description. The conceptual basis of the calculations, as before in our work on other trinuclear clusters,[5-7] is the "clusters in molecules" idea. The results for any given stage of ligation of the $M_3$ cluster are resolved into contributions from ligand orbitals and from MO's of the $M_3$ cluster (rather than individual atomic orbitals of the M atoms). In this way the existence and bonding characteristics of the $M_3$ cluster as a central entity surrounded by ligands are kept clearly at the center of attention. The orbital energies given in tables and diagrams are, as in previous papers reporting related calculations, referred to the energy of a noninteracting metal d orbital as zero. The actual energy of such an orbital in $Mo_3O(OH)_{10}$ according to the final Fock matrix was −8.3 eV.

To implement this "clusters in molecules" approach we begin, naturally, with a calculation of the MO's for the bare cluster, e.g., $Mo_3^{12+}$ with an Mo–Mo distance of 2.529 Å, in this case. Only the five d orbitals of each metal atom play any significant role in the bonding, and these give rise to the set of 10 MO's listed in Table I; for the bare cluster the symmetry is $D_{3h}$ and the MO's are designated accordingly. This symmetry (and the notation) will change to $C_{3v}$ as soon as ligands are added. It can be seen from Table I that the two most strongly bonding (and occupied) MO's are $1a_1'$ and $1e'$, which arise almost entirely as combinations of atomic $d_{z^2}$ and $d_{xz}$ orbitals, respectively. In general, the entire picture of the bare $Mo_3^{12+}$ cluster is the same as that obtained before[5-7] at somewhat different Mo–Mo distances.

Table I. Molecular Orbitals Formed from 4d Orbitals in the $Mo_3^{12+}$ Cluster

| orbital | rel energy, eV | $d_{z^2}$ | $d_{x^2-y^2}$ | $d_{xy}$ | $d_{xz}$ | $d_{yz}$ | s | p |
|---|---|---|---|---|---|---|---|---|
| $1a_2'$ | 6.47 | | | | 84 | | | 16 |
| $2e''$ | 3.40 | | | 14 | | 83 | | 3 |
| $3e'$ | 3.30 | 91 | 3 | | 0 | | 2 | 4 |
| $1a_1''$ | 2.51 | | | 100 | | | | |
| $2e'$ | −1.66 | 2 | 87 | | 8 | | 2 | 1 |
| $1e''$ | −1.97 | | | 85 | | 15 | | 0 |
| $2a_1'$ | −2.45 | 0 | 99 | | | | 1 | 0 |
| $1a_2''$ | −4.57 | | | | | 99 | | 1 |
| $1e'$ | −5.60 | 2 | 8 | | 84 | | 3 | 3 |
| $1a_1'$ | −7.39 | 92 | 0 | | | | 3 | 5 |

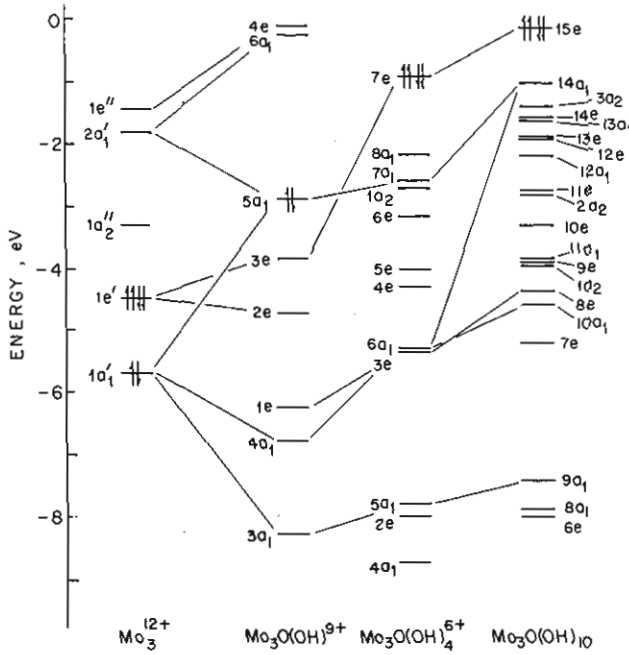


**Figure 2.** Energy levels, calculated in the Fenske–Hall approximation, for the bare $Mo_3^{12+}$ cluster (left), for two intermediate stages of ligand addition, and for the final complete model molecule, $Mo_3(\mu_3\text{-}O)(\mu_3\text{-}OH)(\mu\text{-}OH)_3(OH)_6$. The true calculated energies of all orbitals in the full molecule are 8.3 eV lower than those shown. Thus the first IP of the molecule should be ca. 8.5 eV.

The MO's were calculated for each of the intermediate stages of ligation of the cluster, i.e., for $[Mo_3(\mu_3\text{-}O)(\mu_3\text{-}OH)]^{9+}$ and $[Mo_3(\mu_3\text{-}O)(\mu_3\text{-}OH)(\mu\text{-}OH)_3]^{6+}$, as well as for the final complete molecule, $[Mo_3(\mu_3\text{-}O)(\mu_3\text{-}OH)(\mu\text{-}OH)_3(OH)_6]$. The progressive spreading of the cluster MO's into the total electronic structure of the molecule as a whole can thus be followed step by step. We shall not report all these intermediate results in detail here, but we shall look selectively at a few key aspects and then at the final result. More details are available from the authors on request.

At the left of Figure 2 are shown the lowest five cluster MO's at the energies they have after interacting with $\mu_3$-O

(8) Chisholm, M. H.; Folting, K.; Huffman, J. C.; Kirkpatrick, C. C. *J. Am. Chem. Soc.* **1981**, *103*, 5967.
(9) Hall, M. B.; Fenske, R. F. *Inorg. Chem.* **1972**, *11*, 768.

Table II. Molecular Orbitals for $Mo_3(\mu_3\text{-}O)(\mu_3\text{-}OH)(\mu\text{-}OH)_3(t\text{-}OH')_3(t\text{-}OH'')_3$[a,b]

| orbital | rel energy, eV | $\mu_3$-O | $\mu_3$-OH | $\mu$-OH | t-OH′ | t-OH″ | $Mo_3$ | above 3% |
|---|---|---|---|---|---|---|---|---|
| $5a_2$ | 4.97 | 0 | 0 | 2 | 5 | 3 | 90 | 87% $1a_2'$ |
| 17e | 3.41 | 8 | 5 | 0 | 7 | 3 | 77 | 39% 2e′ + 34% 3e′ |
| $4a_2$ | 1.94 | 0 | 0 | 0 | 8 | 10 | 82 | 82% $1a_1''$ |
| 16e (LUMO) | 1.34 | 2 | 2 | 6 | 11 | 9 | 70 | 58% 1e′ + 10% 2e″ |
| 15e (HOMO) | −0.17 | 2 | 1 | 6 | 12 | 32 | 46 | 36% 1e′ + 8% 3e′ |
| $14a_1$ | −1.05 | 38 | 2 | 0 | 10 | 4 | 46 | 30% $1a_1'$ + 5% $1a_2''$ + 8% $2a_1$ |
| $3a_2$ | −1.44 | 0 | 0 | 0 | 0 | 89 | 12 | 7% $1a_1''$ + 5% $1a_2'$ |
| 14e | −1.63 | 21 | 0 | 2 | 3 | 51 | 22 | 10% 1e′ + 3% 1e″ + 4% 3e′ |
| $13a_1$ | −1.65 | 15 | 0 | 0 | 1 | 75 | 9 | 4% $1a_1'$ |
| 13e | −1.92 | 3 | 9 | 3 | 1 | 73 | 11 | |
| 12e | −1.92 | 1 | 62 | 0 | 25 | 7 | 5 | |
| $12a_1$ | −2.25 | 19 | 0 | 7 | 54 | 9 | 10 | 7% $1a_1'$ |
| 11e | −2.79 | 8 | 2 | 16 | 58 | 3 | 12 | 9% 1e″ |
| $2a_2$ | −2.85 | 0 | 0 | 0 | 86 | 1 | 13 | 10% $1a_1''$ + 3% $1a_2'$ |
| 10e | −3.35 | 30 | 9 | 18 | 8 | 6 | 27 | 8% 1e′ + 4% 1e″ + 11% 2e′ |
| $11a_1$ | −3.92 | 0 | 0 | 85 | 7 | 1 | 6 | 5% $2a_1'$ |
| 9e | −3.95 | 5 | 5 | 4 | 59 | 7 | 19 | 8% 1e″ + 3% 2e′ + 4% 3e′ + 3% 2e″ |
| $1a_2$ | −3.95 | 0 | 0 | 90 | 0 | 0 | 10 | 4% $1a_2'$ + 6% $2a_2'$ |
| 8e | −4.42 | 2 | 0 | 51 | 12 | 1 | 34 | 25% 1e′ + 4% 1e″ + 1% 2e′ |
| $10a_1$ | −4.66 | 13 | 0 | 3 | 25 | 8 | 50 | 42% $1a_1'$ + 3% $1a_2''$ + 5% $2a_1'$ |
| 7e | −5.27 | 0 | 0 | 71 | 3 | 4 | 21 | 4% 2e′ + 7% 3e′ + 7% 5e′ |
| $9a_1$ | −7.47 | 0 | 77 | 1 | 12 | 1 | 9 | 4% $2a_2''$ |
| $8a_1$ | −7.92 | 2 | 0 | 2 | 5 | 77 | 16 | 4% $1a_2''$ + 7% $4a_1'$ |
| 6e | −8.04 | 1 | 0 | 4 | 3 | 73 | 19 | 5% 2e′ + 5% 2e″ + 6% 4e′ |
| 5e | −9.57 | 0 | 0 | 54 | 23 | 3 | 20 | 7% 1e′ + 6% 2e″ + 4% 4e′ |
| $7a_1$ | −9.80 | 1 | 4 | 28 | 42 | 3 | 21 | 10% $1a_2''$ + 2% $2a_1'$ + 4% $3a_1'$ |
| 4e | −10.03 | 0 | 0 | 26 | 52 | 0 | 20 | 3% 1e′ + 3% 2e′ + 4% 3e′ + 6% 2e″ |
| $6a_1$ | −10.66 | 0 | 4 | 50 | 24 | 0 | 22 | 5% $1a_1'$ + 4% $1a_2''$ + 13% $2a_1'$ |

[a] t-OH′ are on the $\mu_3$-O side; t-OH″ are on the $\mu_3$-OH side. [b] The actual (calculated) energies are 8.3 eV lower.

and $\mu_3$-OH. In the next column, moving toward the right, are the central MO's of the $Mo_3O(OH)^{9+}$ unit. Omitted are the $1a_1$ and $2a_1$ MO's, which are O–H and oxygen 2s orbitals of $\mu_3$-OH and $\mu_3$-O, respectively. Tie lines between the first two columns show the principal ways in which the $Mo_3^{12+}$ orbitals contribute to the $Mo_3O(OH)^{9+}$ Mo's. The $3a_1$ and 2e orbitals are mainly responsible for $Mo_3$ to $\mu_3$-OH bonding, while the $4a_1$ and 1e orbitals carry most of the $Mo_3$ to $\mu_3$-O bonding. The metal–metal bonding is principally carried by the 3e and $5a_1$ orbitals, which have 68% and 72% metal character, respectively. The $5a_1$ orbital is the HOMO.

With the addition of the three $\mu$-OH ligands we get the array of orbitals shown in the next column of Figure 2. Not shown are the $1a_1$, $2a_1$, 1e, and $3a_1$ MO's that lie in the range −22.2 to −22.6 eV. The first three are essentially O–H bonding orbitals, and $3a_1$ is essentially the 2s orbital of $\mu_3$-O. All of the virtual orbitals now lie at energies above those shown, and the HOMO is the 7e orbital. This is by far the major e-type contributor to metal–metal bonding. The $a_1$ component of metal–metal bonding is shared by the $7a_1$ and $6a_1$ MO's.

The calculation for the entire $Mo_3O(OH)_{10}$ molecule gave results that are shown, in part, at the right side of Figure 2 and listed in Table II. Between −29.7 and −21.1 eV are all of the MO's that are principally O–H bonding in nature and made up mainly of oxygen 2s and hydrogen 1s atomic orbitals, and the 2s orbital of the $\mu_3$-O atom, with essentially no metal orbital contribution. These are $1a_1$, $2a_1$, $3a_1$, $4a_1$, $5a_1$, 1e, 2e, and 3e.

The molecular orbitals responsible for the Mo–O bonds and oxygen lone pairs are distributed through the energy range −10.7 to −1.4 eV, as can be seen in Table II. In most cases the provenance of these MO's in the O, OR, and $Mo_3$ moieties is so mixed that no simple description of their bonding role is possible. Notable exceptions are the $a_2$ orbitals. The $1a_2$ orbital is a weakly bonding but mainly lone-pair orbital on the $\mu$-OH groups. It lies mainly in the $Mo_3(\mu\text{-}O)_3$ plane. The $2a_2$ and $3a_2$ MO's are occupied by what are essentially lone pairs on the terminal OH oxygen atoms.

We turn now to some of the orbitals that will be most pertinent to a discussion of the metal-to-metal bonding, the redox chemistry, and the electronic absorption spectrum of the compound. These orbitals, shown in Figure 3, are the 15e, 16e, $10a_1$, and $14a_1$ orbitals. To fully convey their spatial characteristics, each one is represented by contours in the $Mo_3$ plane and by a section perpendicular to this plane and including either two metal atoms (e orbitals) or a vertical mirror plane ($a_1$ orbitals).

Metal-to-metal bonding is somewhat distributed over two $a_1$- and several e-type orbitals. The e component of M–M bonding receives its largest contribution from the HOMO, the 15e orbital, but significant contributions also come from the 10e and 8e orbitals. The $a_1$ component of M–M bonding is derived in part from the second-highest filled orbital, $14a_1$, but also, to an even greater extent, from the $10a_1$ orbital. Both of these $a_1$ orbitals, but especially the $14a_1$ orbital, are also significantly involved in bonding of the $Mo_3$ cluster to the $\mu_3$-O atom.

The LUMO, 16e, comes close to having a nodal plane coincident with the $Mo_3$ plane. This is because its parentage is largely in e″-type orbitals of the bare $Mo_3$ cluster, and these (in the $D_{3h}$ symmetry of the bare $Mo_3$ cluster) have a rigorous nodal plane. Thus, while the HOMO is an e orbital of essentially $\sigma$ Mo–Mo bonding type, the LUMO is an e orbital of essentially $\pi$ Mo–Mo bonding type. The LUMO, however, is markedly antibonding with respect to all of the Mo–($\mu_3$-O), Mo–($\mu_3$-OH), and Mo–(OH) bonds.

In Table III are presented the Mulliken populations of the canonical cluster orbitals at each stage of the process of ligating the cluster. It is seen that after an initial drop when the $\mu_3$-O and $\mu_3$-OH ligands are added, the $1a_1'$ and 1e′ cluster orbitals continue to be well populated, and thus they constitute a continuing and principal source of metal–metal bonding throughout. The average charge per metal atom in the neutral molecule is approximately 1+, which is a reasonable value for metal atoms formally in oxidation state 4+ and combined with relatively electronegative oxygen atoms.

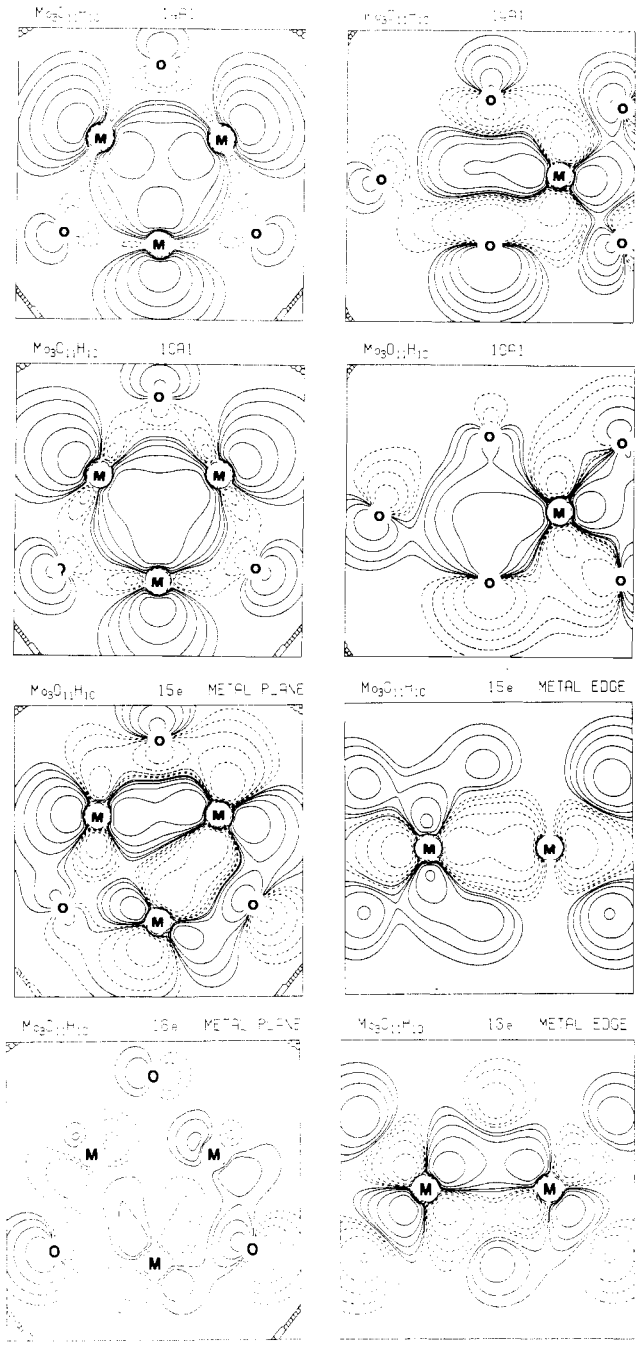


**Figure 3.** Contour diagrams for the wave functions of several important molecular orbitals of $Mo_3O(OH)_{10}$. Positive and negative regions are represented by full and broken lines, respectively. Contours begin at 0.005 e Å$^{-3}$ and increase by a factor of 2 at each step. For each of the orbitals 15e and 16e, contours are shown in the $Mo_3$ plane and in a perpendicular section that contains one Mo–Mo bond. For each of the orbitals $10a_1$ and $14a_1$, there is an in-plane contour and a perpendicular one corresponding to a vertical plane of symmetry.

**Some Predictions.** It is to be noted that the HOMO–LUMO gap is not large, ca. 1.5 eV. (1) This should mean that either oxidation or reduction, or both, should be chemically feasible processes for compounds of this class. For either process the resulting ion should have an electron in an e orbital. (2) The characters of both HOMO (15e) and LUMO (16e) are such that significant structural changes might be expected upon either oxidation or reduction. Thus, while these processes might be achievable at relatively low potentials, they might well be expected to lack reversibility. (3) Because of the low symmetry a considerable number of formally allowed one-electron transitions are to be expected. Some of these should be found in the visible region, and several might well be strong. We shall return to this question in more detail when the observed spectrum is discussed.

Table III. Mulliken Populations and Charges

| | $Mo_3^{12+}$ | $Mo_3O_2H^{9+}$ | $Mo_3O_5H_4^{6+}$ | $Mo_3O_{11}H_{10}$ |
|---|---|---|---|---|
| $1a_1'$ | 2 | 1.66 | 1.76 | 1.78 |
| $1e'$ | 4 | 3.97 | 3.65 | 3.69 |
| $1a_2''$ | | 0.72 | 0.70 | 0.70 |
| $2a_1'$ | | 0.84 | 0.83 | 0.78 |
| $1e''$ | | 0.99 | 1.00 | 1.41 |
| $2e'$ | | 0.97 | 1.10 | 1.23 |
| $1a_1''$ | | 0.00 | 0.00 | 0.35 |
| $3e'$ | | 0.01 | 1.28 | 1.23 |
| $2e''$ | | 0.31 | 0.63 | 1.17 |
| $1a_2'$ | | 0.00 | 0.16 | 0.23 |
| charge on Mo atom | 4.00+ | 2.76+ | 1.74+ | 1.09+ |

**An Alternate, Qualitative View of the Metal–Metal Bonding.** We first note that the structure (Figure 1) we are dealing with can be constructed from three distorted $MoO_6$ octahedra fused along one common edge, thus having two vertices (the $\mu_3$-O and $\mu_3$-OR groups) common to all three octahedra. If we neglect the distortions, each metal atom may be said to use two d orbitals in Mo–O $\sigma$ bonding (the $e_g$ orbitals in an ideal octahedron) and then to have three more d orbitals (the $t_{2g}$ orbitals of an ideal octahedron) available to contain the two d electrons and to be employed in both Mo–Mo bonding and Mo–O $\pi$ bonding. If we ignore the latter, as a first approximation, we may use the three sets of "$t_{2g}$"-type d orbitals to construct molecular orbitals that can be used for metal–metal bonding.

In the spirit of the concept that the bonding or antibonding character of the resulting MO's will be proportional to the magnitudes of the overlaps (positive or negative, respectively) and with a few necessary but trivial coordinate transformations to obtain overlap expressions that are related to the types available in tables,[10] the relative energies of the resulting orbitals were estimated. We also used $D_{3h}$ symmetry since a conjunction of ideal octahedra would yield this rather than the actual $C_{3v}$ symmetry. In this way we get the following three-center MO's, which are listed in order of increasing energy (those of M–M antibonding character carry an asterisk):

$$a_1' \leq e' < e'' < a_1^* < e'^* \leq a_2'^*$$

This sequence of orbitals is in good agreement with those listed in Table I. In the order given above they correspond to the $1a_1'$, $1e'$, $1e''$, $1a_1''$, $3e'$, and $1a_2'$ orbitals of the $Mo_3^{12+}$ cluster. The first three correspond crudely to the $14a_1$, 15e, and 16e orbitals of the complete $Mo_3O(OH)_{10}$ molecule. Thus, even this very drastically simplified approach to the bonding suggests, correctly, that the metal–metal bonding is accomplished by six electrons occupying an $a_1$ + e pair of orbitals of bonding character and that the lowest empty MO of significant metal d orbital parentage (also bonding in the M–M sense) is also an e-type orbital, but one of approximately $\pi$ symmetry relative to the molecular plane.

There may be those who would question the value of the preceding exercise in drastically simplified bonding analysis. We believe it adds a sense of qualitative or intuitive reality that enhances confidence in the more quantitative results. We may now turn to some experimental results that ought to be in harmony with the theoretical picture just developed.

(10) See the following references for further explanation of the procedure: (a) Cotton, F. A.; Haas, T. E. *Inorg. Chem.* **1964**, *3*, 10. (b) Bursten, B. E.; Cotton, F. A.; Stanley, G. G. *Isr. J. Chem.* **1980**, *19*, 132 (cf. the Appendix).

**Table IV.** Electronic Absorption Spectrum of $Mo_3O(ONe)_{10}$ in Hexane Solution and Suggested Assignments

| observations | | | possible assignments | | | |
|---|---|---|---|---|---|---|
| max, nm | max, eV | $\epsilon$, $M^{-1}$ $cm^{-1}$ | transition | polarizn | energy, eV | intens |
| 693 | 1.79 | 390 | $15e \rightarrow 16e$ ($E' \rightarrow E''$) | $z$ | 1.51 | weak |
| 430 | 2.88 | 570 | $15e \rightarrow 17e$ ($E' \rightarrow E'$) | $xy$ | 3.58 | weak |
| 287 | 4.32 | 25 000 | $14a_1 \rightarrow 17e$ ($A_1' \rightarrow E'$) | $xy$ | 4.46 | strong |
| 240 | 5.17 | 18 000 | $15e \rightarrow 5a_2$ ($E' \rightarrow A_2'$) | $xy$ | 5.14 | strong |

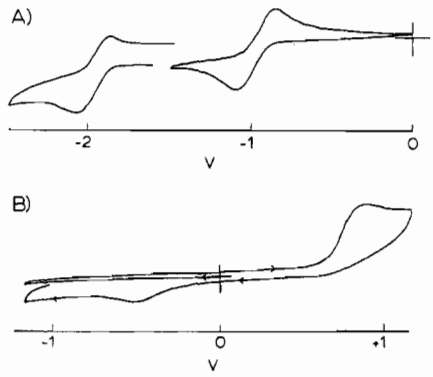


**Figure 4.** Cyclic voltammograms of $Mo_3O(ONe)_{10}$ (V vs. Ag/AgCl): (A) reductive scan in THF; (B) oxidative scan in $CH_2Cl_2$ showing irreversible oxidation at 0.88 V and product wave at ~−0.5 V.

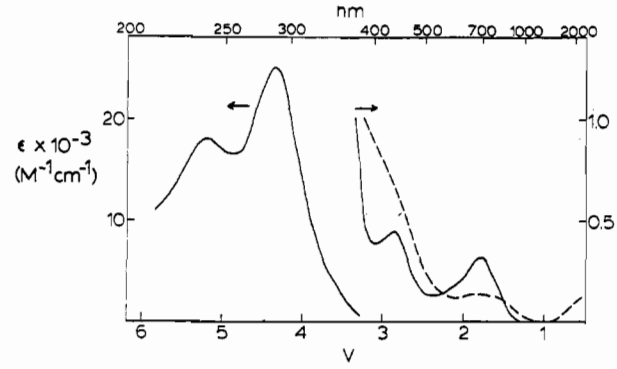


**Figure 5.** Electronic absorption spectra: (—) $Mo_3O(ONe)_{10}$ in hexane; (--) $[Mo_3O(ONe)_{10}]^-$ in THF (0.2 M TBAH).

**Electrochemistry.** The electrochemical properties of $Mo_3O(ONe)_{10}$ were examined in both THF and $CH_2Cl_2$ solutions. In THF, two reductive waves were observed as is illustrated in Figure 4A. The first wave, with $E_{1/2} = -0.91$ V, has a rather large peak separation of 180 mV, indicating some irreversibility to the reduction process. With our experimental setup, reversible couples (such as ferrocene/ferrocenium) exhibited peak separations of 90–120 mV (vs. the 60 mV anticipated), indicating that part of the large separation is due to uncompensated internal resistance.

Reductive coulometry at −1.2 V established that this first wave is a one-electron couple. A subsequent cyclic voltammogram was the same as the initial scan. This implies that the integrity of the complex is maintained during the reduction process. There is, in fact, evidence for fairly long-term stability of the resulting anion. For one thing the reductive and (reverse) oxidative peak heights are equal. It was further shown that even after several hours, oxidative coulometry at 0.0 V regenerated the original species, as determined by electronic absorption spectroscopy.

It thus appears that while the first reduction process is a reversible one, it may be slow because of some energy barrier. According to the electronic structure calculations, the electron must enter an orbital (16e) that has simultaneously metal–metal bonding character and metal–ligand antibonding character; moreover, introduction of an electron into this e-type orbital should lead to distortion, according to the Jahn–Teller theorem. It might thus be that the equilibrium structure of the reduced species differs appreciably from that of the neutral molecule and that a significant barrier must be surmounted to pass from one nuclear configuration to the other.

The second reductive wave, with $E_{1/2} = -1.95$ V, shows a larger peak separation (250 mV) than the first. The similarity in peak heights suggests that it is also a one-electron couple. The oxidative peak height appears to be smaller than that for reduction. Unfortunately, the proximity of this couple to the solvent limit of −2.5 V prevented us from further investigating the properties of the doubly reduced species. No oxidative waves were observed in THF out to the solvent limit of +1.0 V.

The electrochemical properties of $Mo_3O(ONe)_{10}$ in $CH_2Cl_2$ solution are somewhat different. The first reduction occurs at −1.33 V with a peak separation of 220 mV. The second reduction is not observed, apparently occurring beyond the solvent limit of −1.8 V. Moreover, in $CH_2Cl_2$ an oxidation wave is observed and this is shown in Figure 4B. The oxidative peak is at $E = +0.88$, and there is a complete absence of a reductive component (even at 500 mV/s), implying that the process is chemically irreversible. A reductive wave is observed to grow in at ~−0.5 V upon cycling through the oxidative wave, but the decomposition product that gives rise to this is not yet identified. Since oxidation should remove an electron from the 15e orbital which is strongly metal–metal bonding, it is reasonable that this might lead to enough disruption of the structure to make the oxidation an irreversible process.

**EPR Spectra.** The electrochemically generated $Mo_3O(ONe)_{10}^-$ species in THF (0.2 M TBAH) exhibited an EPR signal at 77 K. The signal was centered at $g = 2.047$ and could be seen to be anisotropic. Hyperfine coupling to the $^{95,97}Mo$ nuclei ($I = {}^5/_2$, 25.4%) was observed with $A \approx 2.4 \times 10^{-3}$ $cm^{-1}$. The EPR spectrum is being further studied and will be described in more detail in a future report.

**Electronic Absorption Spectrum.** The absorption spectrum for $Mo_3O(ONe)_{10}$ dissolved in hexane is shown in Figure 5, with the band positions and extinction coefficients summarized in Table IV. As can be seen, the relatively simple spectrum consists of two weak bands ($\epsilon \sim 500$) in the visible region and two strong bands ($\epsilon \sim 20\,000$) in the UV. The green color of the complex is understandable in terms of this absorption spectrum.

To determine probable assignments for the observed absorption bands we shall consider the two higher filled orbitals $14a_1$ and 15e and the four lowest virtual orbitals 16e, $4a_2$, 17e, and $5a_2$. We first note that although the total symmetry of the molecule is $C_{3v}$, the $Mo_3$ core has $D_{3h}$ symmetry and there is little mixing between orbitals of different $D_{3h}$ symmetry types for the six orbitals of concern (see Table II). Transitions among them might then be effectively governed by the selection rules of a $D_{3h}$ molecule. On this basis, only four of the possible eight orbital transitions are found to be allowed. These are listed in Table IV along with first-order estimates of the transition energy, which are simply based on orbital energy differences.

Also included in Table IV are qualitative estimates of the relative transition intensities, i.e., strong or weak. The basis for these intensity predictions is as follows. It is seen that the 15e and $5a_2$ orbitals have large contributions from the same

d orbital type ($d_{xz}$), whereas the $a_2$ orbital contains an in-phase combination of the $d_{xz}$ orbitals and the e orbital an out-of-phase combination. These two orbitals will then essentially differ from one another only in respect to a single symmetry plane: one orbital will be symmetric with respect to this plane while the other will be antisymmetric. Since transitions between orbitals that differ from one another simply by behavior with respect to a symmetry plane are strongly allowed (e.g., atomic s ↔ p, p ↔ d, etc. transitions), it is expected that the 15e → $5a_2$ should be strongly allowed. The same argument holds for the $14a_1$ → 17e transition since both orbitals have heavy contributions from the $d_{z^2}$ orbitals.

The remaining two transitions are seen to be between molecular orbitals that are built up of different types of metal d orbitals: 15e($d_{xz}$) → 16e($d_{xy}$) and 15e($d_{xz}$) → 17e($d_{z^2}$, $d_{x^2-y^2}$). For this reason the two orbitals will differ from one another by more than behavior with respect to a single symmetry plane. These transitions should then be relatively weak as are most d → d transitions.

On the basis of the correlation of the predicted energies and intensities with the experimental data, the band assignments listed in Table IV are proposed. We are reasonably confident in the assignments of the two lower energy bands since no other allowed transitions are expected in this region. (The 15e → $4a_2$ (2.11 V) and $14a_1$ → 16e (2.39 V) transitions are forbidden in $D_{3h}$ symmetry though allowed in $C_{3v}$, and the $14a_1$ → $4a_2$ (2.99 V) transition is dipole forbidden in $D_{3h}$ and $C_{3v}$.) The assignments of the two higher energy bands are much more speculative because the possibility of charge-transfer bands has not yet been considered. According to the calculation, the oxygen lone pairs of the terminal alkoxides ($3a_2$ etc.) occur at only slightly lower energies than the metal–metal bonding orbitals $14a_1$ and 15e. Therefore, oxygen (pπ) to metal charge-transfer transitions are also expected to occur in the UV region (e.g., $3a_2$ → 16e at ~2.8 V). Clearly, polarization and/or resonance Raman studies on the absorption bands would be helpful in this regard. A photoelectron spectrum would also be useful in delineating the position of the oxygen lone pairs relative to the metal–metal bonds.

Since the singly reduced complex is stable in solution, it is interesting to consider what changes in the absorption spectra would be expected upon addition of an electron to the 16e orbital. First, two new low-energy transitions would be expected to appear: 16e → $4a_2$ (0.60 V) and 16e → 17e (2.07 V). Both of these are allowed in the idealized $D_{3h}$ symmetry, the former being *xy* polarized and the latter *z*. Second, since the 16e orbital is now partially occupied, the 15e → 16e transition might decrease in intensity.

A comparison of the spectra of the neutral and reduced species is shown in Figure 4. The reduced complex exhibits a new band at quite low energy (≤0.6 V), which could be assigned to the anticipated 16e → $4a_2$ transition. The 15e → 16e transition of ~1.8 V is observed to lose intensity as expected and also appears to broaden somewhat. Whether the 16e → 17e transition is responsible for this broadening or for the increased absorption at ~3 V is uncertain. Overall, however, the observed spectral changes are quite consistent with the added electron entering the 16e orbital.

**Acknowledgment.** We are grateful to the Robert A. Welch Foundation (Texas A&M University) and the Office of Naval Research (Indiana University) for financial support. We thank Prof. B. E. Bursten of The Ohio State University for helpful discussions.

**Registry No.** $Mo_3O(OH)_{10}$, 88644-53-5; $Mo_3O(ONe)_{10}$, 79210-00-7.

---

Contribution from the Department of Chemistry and Molecular Structure Center, Indiana University, Bloomington, Indiana 47405

# The Molybdenum–Molybdenum Triple Bond. 14.[1] Preparation and Characterization of Mixed Alkoxy–Thiolate Compounds of Formula $Mo_2(OR)_2(SAr)_4$ (M≡M)

MALCOLM H. CHISHOLM,* JAMES F. CORNING, and JOHN C. HUFFMAN

*Received June 24, 1983*

Hydrocarbon solutions of $Mo_2(NMe_2)_6$ react with mesitylenethiol (ArSH) to give $Mo_2(NMe_2)_2(SAr)_4$. Similarly, the alkoxides $Mo_2(OR)_6$ react with mesitylenethiol in hydrocarbon solvents to give $Mo_2(OR)_2(SAr)_4$ compounds, where R = *t*-Bu, *i*-Pr, and $CH_2$-*t*-Bu. These arenethiolato compounds are notably less air sensitive than their precursor amides and alkoxides. Solution $^1H$ NMR data are consistent with anti or rapidly interconverting anti and gauche rotamers of ethane-like dimers $(RO)(ArS)_2Mo{\equiv}Mo(SAr)_2(OR)$. In the solid state, $Mo_2(O\text{-}i\text{-}Pr)_2(SAr)_4$ adopts the anti conformation with crystallographically imposed $C_i$ symmetry and the following important structural parameters: Mo–Mo = 2.230 (1) Å, Mo–S = 2.32 (1) Å (averaged), Mo–O = 1.878 (2) Å, Mo–Mo–S = 95.4 (1)° and 99.8 (1)° and Mo–Mo–O = 106.8 (1)°. Crystal data at −163 °C: $a$ = 21.778 (2) Å, $b$ = 8.600 (2) Å, $c$ = 24.587 (2) Å, $\beta$ = 108.90 (1)°, and $Z$ = 4 in the space group $C2/c$.

## Introduction

Homoleptic compounds of formula $X_3Mo{\equiv}MoX_3$ are known for X = bulky β-elimination-stabilized alkyls ($CH_2CMe_3$, $CH_2SiMe_3$), $NMe_2$, and OR (R = a bulky alkyl or trialkylsilyl group, e.g. *t*-Bu, *i*-Pr, $CH_2$-*t*-Bu, $SiMe_3$, $SiEt_3$, etc.).[2,3] We have wondered for some time whether this series could be extended to include thiolato (mercaptido), SR, ligands. Though there was no reason to believe that such compounds could not exist, our initial synthetic attempts were thwarted by problems arising from molybdenum's high affinity for sulfur, facile C–S bond cleavages, polymerization by μ-SR formation and oxidation of the $Mo_2^{6+}$ center.[4] We were able, however, to attach two SR ligands to the $(Mo{\equiv}Mo)^{6+}$ unit

(1) Chisholm, M. H.; Folting, K.; Huffman, J. C.; Ratermann, A. R. *Inorg. Chem.* **1984**, *23*, 613.
(2) Cotton, F. A.; Walton, R. A. In "Multiple Bonds Between Metal Atoms"; Wiley-Interscience: New York, 1982.
(3) Chisholm, M. H.; Cotton, F. A. *Acc. Chem. Res.* **1978**, *11*, 356.
(4) Chisholm, M. H.; Corning, J. F.; Huffman, J. C. *Inorg. Chem.* **1982**, *21*, 286.

0020-1669/84/1323-0754$01.50/0 